

A unified theoretical framework for Kondo superconductors: Periodic Anderson impurities with attractive pairing and Rashba spin-orbit coupling

Shangjian Jin,^{1,2} Darryl C. W. Foo,² Tingyu Qu,¹ Barbaros Özyilmaz,^{1,2,3} and Shaffique Adam^{3,4}

¹*Department of Physics, National University of Singapore, 2 Science Drive 3, 117551 Singapore*

²*Centre for Advanced 2D Materials, National University of Singapore, 6 Science Drive 2, 117546 Singapore*

³*Department of Materials Science and Engineering, National University of Singapore, 9 Engineering Drive 1, Singapore 117575*

⁴*Department of Physics, Washington University in St. Louis, St. Louis, Missouri 63130, United States*

(Dated: September 20, 2024)

Magnetic superconductors manifest a fascinating interplay between their magnetic and superconducting properties. This becomes evident, for example, in the significant enhancement of the upper critical field observed in uranium-based superconductors, or the destruction of superconductivity well below the superconducting transition temperature T_c in cobalt-doped NbSe₂. In this work, we argue that the Kondo interaction plays a pivotal role in governing these behaviors. By employing a periodic Anderson model, we study the Kondo effect in superconductors with either singlet or triplet pairing. In the regime of small impurity energies and high doping concentrations, we find the emergence of a Kondo resistive region below T_c . While a magnetic field suppresses singlet superconductivity, it stabilizes triplet pairing through the screening of magnetic impurities, inducing reentrant superconductivity at high fields. Moreover, introducing an antisymmetric spin-orbital coupling suppresses triplet superconductivity. This framework provides a unified picture to understand the observation of Kondo effect in NbSe₂ as well as the phase diagrams in Kondo superconductors such as UTe₂, and URhGe.

PACS number(s): 74.20.Fg, 74.20.Rp, 74.25.Dw

I. INTRODUCTION

The intricate interplay between magnetism and superconductivity has garnered significant attention due to the competition of magnetic and superconducting ground states. Various lanthanum-based heavy fermion singlet superconductors [1–4] have shown a second transition temperature T_K where a resistive state resurfaces due to the Kondo effect that disrupts superconductivity [5, 6]. More recently, there has been a surge of interest in uranium-based ferromagnetic heavy fermion superconductors such as URhGe, UCoGe, and UTe₂ for their potential to realize spin triplet superconductivity with non-trivial topological properties [7–11]. These compounds hold promise as candidates for a Kondo-effect-induced topological superconductors [12–15]. Moreover, the hybridization between itinerant electrons and localized $5f$ electrons of uranium atoms allows for a coexistence of the Kondo effect and superconductivity that was predicted theoretically [16–19], and confirmed experimentally [13, 20, 21]. This underscores the importance of the Kondo interaction in elucidating the $B - T$ phase diagram of U-based superconductors. The phase diagrams of these materials exhibit diverse features: URhGe displays high-field reentrant superconductivity with the magnetic field $\mathbf{B} \parallel b$ -axis [22]; UCoGe shows an S-shaped upper critical field [23]; and UTe₂ exhibits a large upper critical field [12], significant field anisotropy, field reentrant superconductivity [24], and multiple SC phases under pressure [25].

In a separate development, few layer transition metal dichalcogenides have recently emerged as a feasible and customizable platform conducive to two-dimensional Kondo superconductivity, explored both experimentally [26, 27] and theoretically [28–30]. For example, in a recent experiment [31], NbSe₂ encapsulated by atomically-thin boron nitride was interfaced with magnetic dopants introduced by e-

beam evaporation of Co. The observed destruction of superconductivity concomitant with a logarithmic resistance-temperature behavior was attributed to the Kondo effect. In this work, we refer to this platform as Co-NbSe₂. We note that the superconducting state of few-layers NbSe₂ is intrinsically parity mixed due to Ising spin-orbit coupling [32–37]. It is believed that manipulating the Kondo effect in NbSe₂ through doping concentration, temperature, and magnetic field could pave the way for constructing pure triplet superconducting spintronic devices (see e.g. Ref. [38]).

Despite the similarity in the underlying physics of these different systems, to our knowledge there is no unified microscopic theory to explain the diverse $B - T$ phase diagrams observed in materials ranging from Co-NbSe₂ to U-based superconductors. This is the goal of the present work. Before we outline our model, we briefly discuss what is known in the theoretical literature. More than fifty years ago, Müller-Hartmann and Zittartz [5] predicted the destruction of superconductivity by the Kondo effect using the Nagaoka approach. This mechanism fails below the Kondo temperature and always predicts superconductivity independent of the impurity concentration. About 20 years ago, Barzykibn and Gor'kov [6] studied the Kondo effect in s-wave superconductors using a periodic Anderson model elucidating the relationship between T_c and the impurity concentration for Ce_{1-x}La_xRu₃Si₂, but they did not consider the effect of magnetic fields. Almost five years ago, Suzuki and Hattori [17] explored a possible connection between Kondo coupling and reentrant triplet superconductivity using a one-dimensional Kondo lattice model. More recent work by Machida [39] established a Ginzburg-Landau theory considering the rotation of the triplet order parameter $\mathbf{d}_{\mathbf{k}}$ vector to qualitatively determine the B_{c2} shape in URhGe, UCoGe and UTe₂, while assuming a temperature-dependent absolute upper field limit. It is in this context that we develop a comprehensive theory ca-

pable of capturing the roles of magnetic impurities and magnetic fields in both singlet and triplet superconductors to understand the diverse patterns of superconductivity destruction and reentrance across different materials.

To this end, we start with a periodic Anderson model to investigate the pair-breaking process in superconductors. Utilizing the Bardeen–Cooper–Schrieffer (BCS) weak coupling assumption and Green’s function approach, we solve the gap equations and derive pair-breaking equations. For both singlet and triplet superconductors, this formalism predicts a second transition T_K back to a normal state for a range of doping concentrations. We are then able to incorporate both an external magnetic field and spin-orbit coupling. This allows us to extract the phase-diagrams for a range of materials and predict some unexpected phenomena such as reentrant superconductivity for singlet superconductors, and the enhancement of T_c with magnetic fields for triplet superconductors.

II. PERIODIC ANDERSON MODEL

We start with the periodic Anderson model, a standard approach for describing many transition metal, rare-earth, and heavy fermion systems [15, 40–42]

$$H_0 = \sum_{\mathbf{k},s} \varepsilon_{\mathbf{k}} c_{\mathbf{k}s}^\dagger c_{\mathbf{k}s} + \sum_{i,s} \varepsilon_f f_{is}^\dagger f_{is} + \frac{U}{2} \sum_i f_{i\uparrow}^\dagger f_{i\downarrow}^\dagger f_{i\downarrow} f_{i\uparrow}. \quad (1)$$

Here $c_{\mathbf{k}s}^\dagger$ ($c_{\mathbf{k}s}$) and f_{is}^\dagger (f_{is}) are the creation (annihilation) operators for the conduction electrons and the localized f -electrons, respectively. $\varepsilon_{\mathbf{k}}$ is the conduction band dispersion and ε_f denotes the impurity energy level. Both $\varepsilon_{\mathbf{k}}$ and ε_f are defined relative to the Fermi level. Since the repulsive on-site Coulomb potential is very strong for the f -electrons, we take it to be infinite in this work. This is the Kondo limit where the doubly occupied f -electron states are projected out and the effective energy $\varepsilon_f < 0$ [15, 43]. The hybridization between the local and conduction electrons can be written as

$$H_{cf} = \sum_{i,\mathbf{k},s} \left(\sqrt{x} V e^{i\mathbf{k}\cdot\mathbf{R}_i} f_{is}^\dagger c_{\mathbf{k}s} + h.c. \right), \quad (2)$$

where the hybridization V is assumed to be \mathbf{k} -independent for simplicity. Importantly, we have introduced $x = \langle f_i^\dagger f_i \rangle$ that allows us to change the f -electrons concentration. This corresponds to a virtual crystal approximation where each unit cell is considered to contain f -electrons with concentration x , resulting in an effective hybridization of $\sqrt{x}V$ [6]. When the impurity energy is comparable to $k_B T_{c0}$ (which is much smaller than the bandwidth, on the order of 1 eV), the virtual crystal approximation is identical with the coherent potential

approximation [44, 45] that replaces the inhomogeneous potential of a disordered material with an effective potential.

To study Kondo superconductors, we add an effective attractive superconducting pairing potential in the weak-coupling limit [46]

$$H_{pair} = \frac{1}{2} \sum_{\mathbf{k},\mathbf{k}',s_1,s_2} V_{\mathbf{k}\mathbf{k}'} c_{-\mathbf{k}s_2}^\dagger c_{\mathbf{k}s_1}^\dagger c_{\mathbf{k}'s_1} c_{-\mathbf{k}'s_2}. \quad (3)$$

In this work, we assume a generic attractive potential $V_{\mathbf{p}\mathbf{k}} = -\sum_{l=0}^{\infty} 4\pi V_l \sum_m Y_{lm}(\Omega_{\mathbf{p}}) Y_{lm}^*(\Omega_{\mathbf{k}})$, where $V_l = V_l(k_F, k_F)$ is constant and Y_{lm} are spherical harmonics [47, 48]. Such effective potential gives rise to both spin singlet and triplet pairing, with $l = 0, 1, 2, 3$ for s -, p -, d -, and f -wave superconducting order parameters. Our full Hamiltonian has the form

$$H = H_0 + H_{cf} + H_{ASOC} + H_Z + H_{pair}, \quad (4)$$

where H_{ASOC} allows for an antisymmetric spin-orbit coupling (ASOC) in these compounds caused by the breaking of inversion symmetry,

$$H_{ASOC} = \sum_{\mathbf{k},s_1,s_2} \boldsymbol{\gamma}_{\mathbf{k}} \cdot \boldsymbol{\sigma}_{s_1s_2} c_{\mathbf{k}s_1}^\dagger c_{\mathbf{k}s_2} \quad (5)$$

which is of the Rashba type [32, 49], and the magnetic field is included through a Zeeman field

$$H_Z = \sum_{\mathbf{k},s_1,s_2} \mathbf{B} \cdot \boldsymbol{\sigma}_{s_1s_2} \left(c_{\mathbf{k}s_1}^\dagger c_{\mathbf{k}s_2} + f_{\mathbf{k}s_1}^\dagger f_{\mathbf{k}s_2} \right), \quad (6)$$

where \mathbf{B} is external magnetic field, and $\boldsymbol{\sigma}$ are the Pauli matrices. For simplicity, we set the Landé factor $g = 2$ and use dimensionless variables where $\mu_B = k_B = \hbar = 1$.

III. RESULTS

To determine the superconducting phase diagram, we calculate the superconducting transition temperature T_c by solving the gap equation. Following a Green’s function approach for superconductivity, the linearized gap equation is given by [46]

$$\Delta(\mathbf{p}) = -T \sum_{n,\mathbf{k}} V_{\mathbf{p}\mathbf{k}} G_{cc}(\mathbf{k}, i\omega_n) \Delta(\mathbf{k}) G_{cc}^T(-\mathbf{k}, -i\omega_n), \quad (7)$$

with the gap function $\Delta(\mathbf{k}) = [\psi_{\mathbf{k}} + \mathbf{d}_{\mathbf{k}} \cdot \boldsymbol{\sigma}] i\sigma_y$, where $\psi_{\mathbf{k}}$ ($\mathbf{d}_{\mathbf{k}}$) is the singlet (triplet) order parameter. $G_{cc}(\mathbf{k}, i\omega_n)$ is the normal state Green’s function for conduction electrons, whose expression is shown in Appendix A. For simplicity we assume a spherical Fermi surface in all of our calculations. With this assumption, the mixed singlet and triplet gap equations become decoupled and can be solved separately as shown in Appendix B. The pair-breaking equations determining T_c are then given by

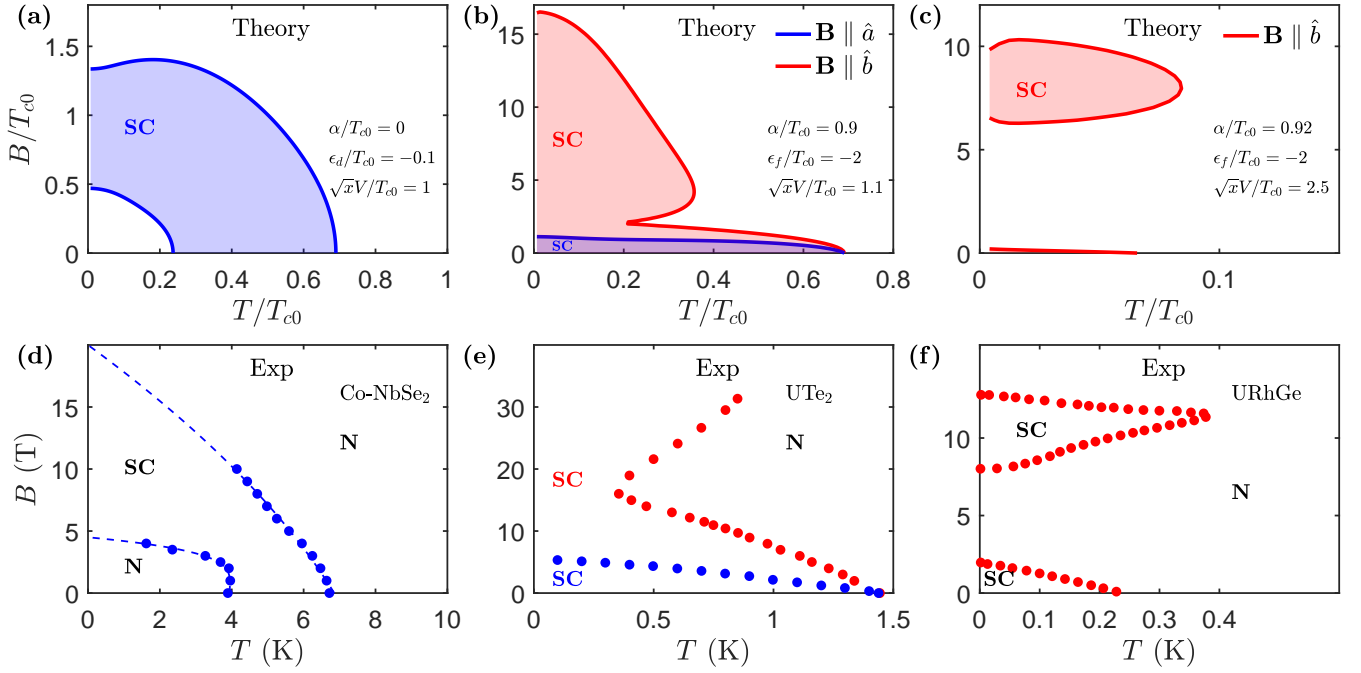


FIG. 1. Theoretical calculation for the superconducting $B - T$ phase diagrams (upper panels) compared with experimental results (bottom panels) for Co-NbSe₂, UTe₂, and URhGe. Qualitative agreement with experiment is achieved within the same theoretical framework. (a) Singlet superconducting boundary that is isotropic in magnetic field. (b) The blue (red) line is the computed triplet superconducting boundary with \mathbf{B} parallel to a -axis (b -axis) using $\boldsymbol{\gamma}_{\mathbf{k}} = \alpha(-k_y, k_x, 0)$ and $\mathbf{d}_{\mathbf{k}} = (k_y + ik_z, k_x, ik_x)$. (c) Triplet superconducting boundary using $\boldsymbol{\gamma}_{\mathbf{k}} = \alpha(0, k_x, 0)$ and $\mathbf{d}_{\mathbf{k}} = (k_z, ik_z, k_x + ik_y)$. (d) The experimental data of Co-NbSe₂ for $\mathbf{B} \parallel ab$ plane is from Ref. [31]. (e) and (f) Data for UTe₂ and URhGe are extracted from Ref. [14] and Ref. [22], respectively.

$$\begin{cases} \ln \frac{T_c}{T_{c0}} = 2\pi T_c \sum_{n=0}^{\infty} \left\langle |\hat{\psi}_{\mathbf{k}}|^2 \frac{\Omega_n [\Omega_n^2 + \frac{1}{4}(\mathbf{b} - \tilde{\mathbf{b}})^2]}{[\Omega_n^2 + \frac{1}{4}(b + \tilde{b})^2][\Omega_n^2 + \frac{1}{4}(b - \tilde{b})^2]} \right\rangle_{\mathbf{k}} - \frac{1}{\omega_n} & \text{for singlet,} \\ \ln \frac{T_c}{T_{c0}} = 2\pi T_c \sum_{n=0}^{\infty} \left\langle \frac{|\hat{d}_{\mathbf{k}}|^2 \Omega_n [\Omega_n^2 + \frac{1}{4}(\mathbf{b} + \tilde{\mathbf{b}})^2] - (\tilde{\mathbf{b}} \cdot \hat{d}_{\mathbf{k}})(\mathbf{b} \cdot \hat{d}_{\mathbf{k}}^*) \Omega_n - i(\hat{d}_{\mathbf{k}} \times \hat{d}_{\mathbf{k}}^*) \cdot i[\frac{1}{2}\Omega_n^2(\mathbf{b} - \tilde{\mathbf{b}}) + \frac{b^2 - \tilde{b}^2}{8}(\mathbf{b} + \tilde{\mathbf{b}})]}{[\Omega_n^2 + \frac{1}{4}(b + \tilde{b})^2][\Omega_n^2 + \frac{1}{4}(b - \tilde{b})^2]} \right\rangle_{\mathbf{k}} - \frac{1}{\omega_n} & \text{for triplet,} \end{cases} \quad (8)$$

where we have introduced

$$\Omega_n = \omega_n + xV^2 \text{Im} \frac{\varepsilon_f - i\omega_n}{(\varepsilon_f - i\omega_n)^2 - B^2} \quad (9)$$

as the Matsubara frequencies shifted by doping, and the effective field

$$\mathbf{b} = \boldsymbol{\gamma}_{\mathbf{k}} + \mathbf{B} \left[1 + \frac{xV^2}{(\varepsilon_f - i\omega_n)^2 - B^2} \right]. \quad (10)$$

Note that $b = \sqrt{\mathbf{b} \cdot \mathbf{b}}$ is a complex number whose argument is limited to $(-\frac{\pi}{2}, \frac{\pi}{2}]$, and we denote $\tilde{\mathbf{b}} = \mathbf{b}(-\mathbf{k}, -i\omega_n)$. The normalized gap functions are $\hat{\psi}_{\mathbf{k}} = \frac{\psi_{\mathbf{k}}}{\sqrt{\langle |\psi_{\mathbf{k}}|^2 \rangle_{\mathbf{k}}}}$ and $\hat{d}_{\mathbf{k}} = \frac{\mathbf{d}_{\mathbf{k}}}{\sqrt{\langle |\mathbf{d}_{\mathbf{k}}|^2 \rangle_{\mathbf{k}}}}$, where the notation $\langle \cdots \rangle_{\mathbf{k}}$ indicates an average over the Fermi surface. The bare superconducting critical temperature $T_{c0}^l = 1.13\omega_D \exp[-\frac{1}{N(0)V_l}]$ for each channel is determined by the strength of effective attractive potential. Finally, we have checked that Eq. (8) reproduces the known results of Sigrist *et al.* [49] in the limit of vanishing Kondo impurities i.e. $x = 0$.

IV. DISCUSSION OF EXPERIMENTAL DATA

A. Singlet Superconductivity

To show the validity of our superconducting model, we first compare the theoretical $B - T$ phase diagrams with experimental data. We note that we just intend to produce the observed B_{c2} qualitatively rather than a quantitative fit to experimental data. A more quantitative approach would require that we relax our assumption of a spherical Fermi surface in favor of a more materials-specific band structure. This is not the goal of the present work, but rather to showcase the diversity of phase diagrams that emerge from our (simplified) theoretical model.

We start with cobalt doped NbSe₂, where Co atoms are introduced by diffusion near the interface and provide localized d -electrons [31]. Previous work suggests that monolayer NbSe₂ supports a mixture of singlet and triplet order parameters due to Ising spin orbit coupling [29, 33, 34] (that quickly decreases with increasing layers recovering in-plane inversion

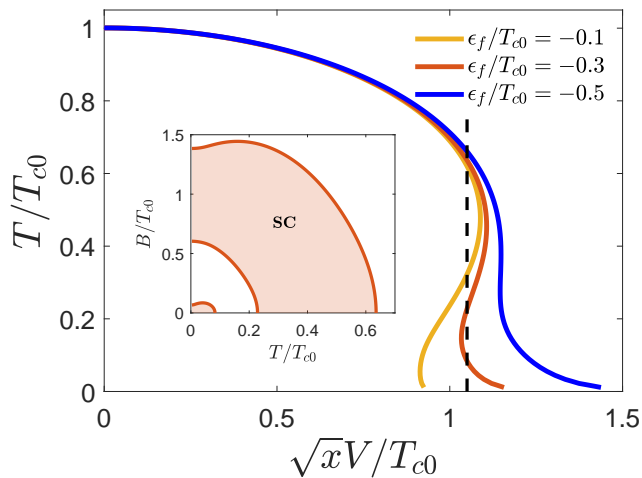


FIG. 2. Singlet superconducting transition temperature as a function of effective Kondo hybridization $\sqrt{x}V$ and impurity energy ε_f in the absence of magnetic field and ASOC. The inset shows the calculated $B - T$ superconducting phase diagram with $\varepsilon_f/T_{c0} = -0.3$ and $\sqrt{x}V/T_{c0} = 1.05$ (corresponding to the orange line at the intersection with the black dashed line).

symmetry [50]). It is therefore appropriate to assume singlet pairing without ASOC in the theory to compare with the ~ 10 layer Co-NbSe₂ experimental data [31]. This is shown in the left panel of Fig. 1, where our theory is shown in panel (a) and the experimental data in panel (d). Both theory and experiment show a window of superconductivity at intermediate magnetic fields and temperature. At low magnetic field and low temperature we find a Kondo phase. Increasing the magnetic field gives reentrant superconductivity – a surprising result for s-wave superconductivity.

We make some further observations: (i) With magnetic impurities, it is possible to have three transition temperatures ($T_{c1} > T_{c2} (T_K) > T_{c3}$); (ii) T_{c1} is suppressed by magnetic doping which is a well-known conclusion [51]; (iii) Without ASOC the superconducting transition is isotropic in \mathbf{B} ; and (iv) In the zero temperature limit and without ASOC, the critical magnetic field can be simplified to

$$\ln \frac{B}{T_{c0}} + \frac{xV^2}{\varepsilon_f^2 + xV^2} \frac{1}{2} \ln \frac{|B^2 - \varepsilon_f^2 - xV^2|}{B^2} - \ln \frac{\pi}{2e^{\gamma_0}} = 0, \quad (11)$$

where γ_0 is Euler's constant.

Figure 2 shows the transition temperatures of singlet superconductors as a function of magnetic doping. Initially, T_c decreases with increasing magnetic doping. However, at higher doping, particularly when the impurity energy $|\varepsilon_f|$ is small, an S-shaped T_c curve emerges. For some impurity concentrations multiple phase transitions are predicted (see the dashed line intersecting the orange line in Fig. 2). The intermediate temperature phase set by $T_{c2} \sim T_K$ yields a resistive state attributed to the Kondo interaction that enhances pair-breaking and disrupts superconductivity. As the temperature is further lowered, a third critical temperature T_{c3} for reentering superconductivity is predicted when the pair-breaking

passes through its maximum and then diminishes, allowing superconductivity to reemerge.

The corresponding $B - T$ phase diagram shows three distinct phases (see the inset of Fig. 2). A Kondo-induced resistive phase is nestled in between two superconducting regions. In the zero temperature limit, the three critical fields given by Eq. (11) satisfy $B_3^c < |\varepsilon_f| < B_2^c < \sqrt{\varepsilon_f^2 + xV^2} < B_1^c$. A maximum of pair-breaking strength is observed at $B = |\varepsilon_f|$, corresponding to the energy required to excite local electrons to the Fermi level. However, when $|\varepsilon_f|$ becomes large, the pair-breaking effect is insufficient to disrupt superconductivity, resulting in a single critical temperature.

We note that in the paramagnetic limit (i.e. the highest critical field B_1^c that breaks superconductivity), the superconducting state is destroyed due to the alignment of electron spins. We find that the paramagnetic limit increases with doping, and exceeds $\sqrt{\varepsilon_f^2 + xV^2}$ (see Fig. 3(a)). As doping increases, T_c decreases while B_1^c rises, and a Kondo-induced resistive state appears. This trend is consistent with experimental observations [31].

B. Triplet Superconductivity

Before we can apply our framework to triplet superconductors, we first need to determine the appropriate order parameter \mathbf{d} and spin-orbit coupling $\gamma_{\mathbf{k}}$. For UTe₂, the pairing symmetry remains controversial despite several attempts to determine it experimentally using specific-heat [52], scanning tunneling microscopy [13], Kerr effect [53], Knight shift [54, 55], and pulse echo ultrasound [56]. For this work, we adopt a more phenomenological approach. For UTe₂ we assume the form $\mathbf{d} = (k_y + ik_z, k_x, ik_x)$ and note that this choice is compatible both with some of the experiments on UTe₂ (e.g. Refs. [13, 57]), and also with theoretical considerations starting from the D_{2h} point group symmetry (e.g. Refs. [46, 58]).

With this choice of \mathbf{d} , we get the lowest upper critical field in the a direction, with a large d_x component. It has a net magnetization $i \langle \mathbf{d} \times \mathbf{d}^* \rangle_{\mathbf{k}}$ along the a -axis (the magnetic easy axis of UTe₂ [8]). Generically, \mathbf{d} does not need to be fixed and could depend on the magnetic field. For example, some recent works [39, 59, 60] consider the rotation of \mathbf{d} in UTe₂ with an applied magnetic field. This possibility is not ruled out by our results, and for $B \gtrsim 20 T$, we expect some alignment of \mathbf{d} with the applied field. However, in this work we focus on the low field regime where the direction of \mathbf{d} is determined only by the easy axis of the UTe₂ crystal. As we observe below, the qualitative agreement between our theory and experimental data indicates that \mathbf{d} vector rotation is not necessary to understand the phase diagram.

It is known that UTe₂ shows a coexistence of Kondo resonance and superconductivity where the Kondo temperature varies from ~ 19.6 K to 26 K [13] and $T_c = 1.6 \sim 2.1$ K depending on sample preparation [12, 55, 61]. The U-5f electrons carry the magnetic moment and therefore $x \equiv 1$. The antisymmetric spin-orbit coupling arising from the local inversion symmetry breaking at uranium atoms [62] is simpli-

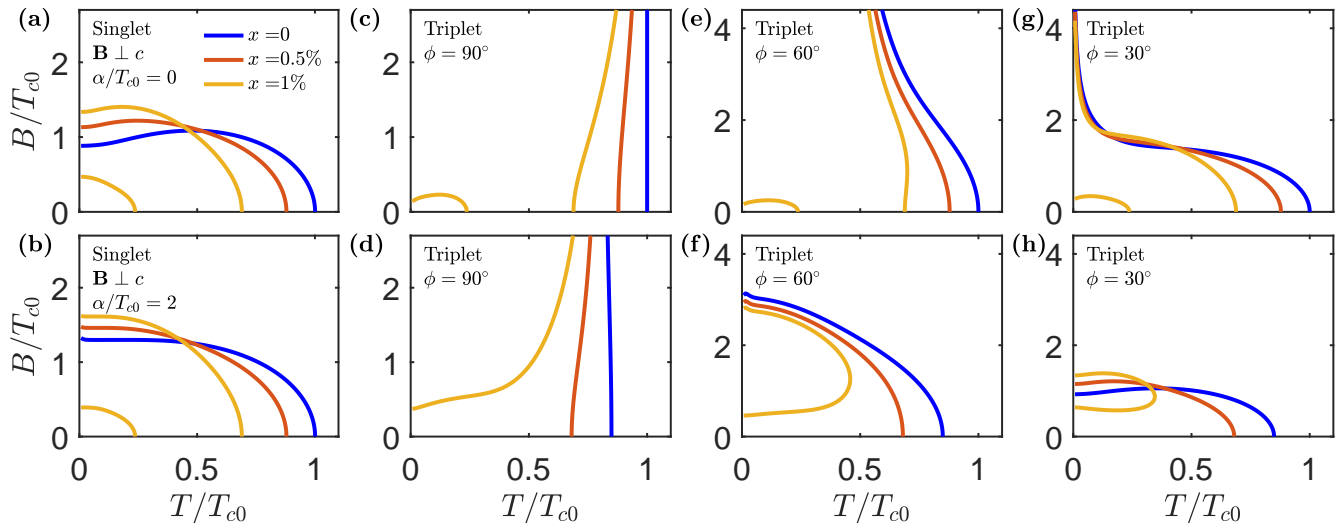


FIG. 3. Evolution of superconducting boundary with magnetic field direction, impurity concentration, and strength of spin-orbit coupling. The calculation utilizes $\varepsilon_f/T_{c0} = -0.1$ and $V/T_{c0} = 10$. ASOC is chosen to break c -axis mirror, $\gamma_{\mathbf{k}} = \alpha(-k_y, k_x, 0)$ with the strength $\alpha/T_{c0} = 0$ (the upper panel) and $\alpha/T_{c0} = 2$ (the bottom panel). (a)-(b) Magnetic field is spatial isotropic in ab plane for singlet pairing. (c)-(h) Influence of magnetic field direction for triplet pairing with $\mathbf{d}_{\mathbf{k}} = (k_y, 0, 0)$. The magnetic field is fixed in ab plane with angle ϕ to a -axis.

fied to $\gamma_{\mathbf{k}} = \alpha(-k_y, k_x, 0)$. The finite strength of ASOC also helps to suppress the triplet superconductivity since it is not parallel to the \mathbf{d} vector.

Fig. 1(b) shows the calculated B_{c2} with $\mathbf{B} \parallel a$ and $\mathbf{B} \parallel b$ using these assumptions. We use a lower impurity energy ε_f to make $T_K > T_c$. For $\mathbf{B} \parallel a$, SC is quickly destroyed due to the large a -component of \mathbf{d} vector. However, we get a L -shaped B_{c2} curve for $\mathbf{B} \parallel b$, where the inflection point happens at $B \approx |\varepsilon_f|$ with the strongest Kondo-induced pair-breaking strength. A higher magnetic field overcomes the corresponding excitation energy and screens out the Kondo effect, resulting in the increase of T_c . We note that in our model the B_{c2} curve along c -axis is slightly higher than that along b -axis, while it is lower than b -axis B_{c2} in the experiment. We attribute this discrepancy to our simplifying assumption of a spherical Fermi surface which does not take into account the large deformation of the density of states caused by the large c lattice constant (see e.g. Ref. [62]). Nonetheless, the qualitative agreement is still very good.

Finally, we look at URhGe. Here we assume $\mathbf{d} = (k_z, ik_z, k_x + ik_y)$. This choice has a net magnetization along the c -axis and is consistent with previous theoretical [63] and experimental [64] work on this material. URhGe exhibits a ferromagnetic (FM) order aligned to the c -axis at Curie temperature $T_{Curie} = 9.5$ K and enters SC phase at $T_c = 0.25$ K with FM state persisting [8]. The field reentrant superconductivity is suggested to be strongly linked to the Kondo interaction [17]. The ASOC of URhGe arises from breaking local inversion symmetry [65, 66] and is taken to be $\gamma_{\mathbf{k}} = \alpha(0, k_x, 0)$. Our results are shown in Fig. 1(c) computed for $\mathbf{B} \parallel b$ -axis, and compared to the measurement Fig. 1(f). We choose a larger hybridization energy than UTe_2 since the bond coupling U-5*f* and Rh-4*p* electrons in URhGe [67] is shorter than for

the U-5*f* and Te-5*p* electrons in UTe_2 [18]. With this strong hybridization, T_c at zero field is significantly suppressed by the Kondo effect. However, this suppression is then mitigated at high fields, leading to a T_c that exceeds its zero-field value. We also see two separate superconducting regions in theory. This is due to antisymmetric spin-orbit coupling that partly enhances the pair-breaking strength and breaks superconductivity around $B = |\varepsilon_f|$. At even higher fields, the Kondo-induced pair-breaking is weakened, leading to the high-field superconducting phase.

V. ADDITIONAL PREDICTIONS OF THE MODEL

We can now explore other possible phase diagrams by varying the parameters in the theory with the hope that these might be observed experimentally in other materials. Assuming that ASOC breaks the c -axis mirror symmetry, we can generically write $\gamma_{\mathbf{k}} = \alpha(-k_y, k_x, 0)$ [32, 49]. For singlet superconductors, we assume a constant superconducting gap ($\hat{\psi}_{\mathbf{k}} = 1$) similar to the results shown in Figs. 3(a) and (b). (We note that the previous results without ASOC holds for any $\hat{\psi}_{\mathbf{k}}$. However, the \mathbf{k} -dependent $\gamma_{\mathbf{k}}$ will be different depending on the singlet order parameter.) The superconductivity remains isotropic with respect to the field direction in the ab plane. T_c at zero field is completely unaffected by ASOC since $\gamma_{-\mathbf{k}} = -\gamma_{\mathbf{k}}$, and the effective field vector \mathbf{b} vanishes in Eq. (8). The upper critical field $B_{c2}(0)$ increases due to the presence of $\gamma_{\mathbf{k}} \not\parallel \mathbf{B}$, which weakens pair-breaking, thereby requiring a higher magnetic field to destroy superconductivity.

For triplet superconductors, we consider a triplet order parameter $\mathbf{d}_{\mathbf{k}} = (k_y, 0, 0)$ with $\langle S_x \rangle = 0$ for simplicity. We focus on the ab plane magnetic field with angle ϕ to the a -axis.

Figures 3(c)-(h) show the $B - T$ phase diagrams of triplet superconductors as a function of magnetic doping and anti-symmetric spin-orbit coupling. T_c at zero field is suppressed by doping as expected. However, surprisingly, T_c is enhanced by the magnetic field when $\mathbf{B} \perp \mathbf{d}_k$ since the magnetic field weakens the Kondo-induced pair-breaking through the $|\hat{d}_k|^2$ term in Eq. (8), screening out the magnetic impurities (see Fig. 3(c) and (d)). To our knowledge, this mechanism for the enhancement of T_c has not been reported previously in the literature.

Rotating the \mathbf{B} direction to the \mathbf{d} direction results in a suppression of the T_c curve (see Figs. 3(e)-(h)). Provided \mathbf{B} is nearly parallel to \mathbf{d} , the increase of $\hat{b} \cdot \mathbf{d}_k^*$ term enhances the pair-breaking and reduces T_c . We can therefore predict the necessary conditions for the existence of $B_{c2}(0)$ at zero temperature: (i) If $\gamma_k \cdot \mathbf{B} = 0$ for all \mathbf{k} , then it requires $\mathbf{d}_k \parallel \mathbf{B}$ for all \mathbf{k} (see the zero ASOC case in Figs. 3(c), (e) and (g), where only $\phi = 0$ gives $B_{c2}(0)$); (ii) If $\gamma_k \cdot \mathbf{B} \neq 0$ for any \mathbf{k} , then $B_{c2}(0)$ exists provided $\mathbf{B} \cdot \mathbf{d}_k \neq 0$ for any \mathbf{k} (see Figs. 3(d), (f) and (h)). This is because ASOC enhances the $\hat{b} \cdot \mathbf{d}_k^*$ term which in turn increases the pair-breaking strength, yielding a zero-temperature upper critical field. We hope that these conditions will help experimentalists correctly identify the pairing symmetry of new and existing triplet superconductors. In sharp contrast to singlet superconductors, the presence of ASOC reduces the zero field triplet T_c , since pair-breaking in the $|\hat{d}_k|^2$ term in Eq. (8) (triplet) is increased.

We predict that higher doping concentrations will make it easier to observe the Kondo resistive state at low temperature in triplet superconductors. In the absence of ASOC, the Kondo phase appears at low magnetic fields, while superconductivity reenters at higher fields. However when ASOC and Kondo hybridization are both strong, pair-breaking is significantly enhanced, completely suppressing superconductivity at zero field (see Figs. 3(d), (f) and (h)). Applying a magnetic field then screens out the magnetic impurities, resulting in a field-induced superconductivity. Enhancing superconductivity with a magnetic field is very unusual. This suggests that materials not typically considered superconducting, but which exhibit a strong Kondo effect and spin-orbit coupling, could potentially be made superconducting through the application of a magnetic field.

Finally, the last term of Eq. (8) (triplet) arises from the non-unitary \mathbf{d} vector, which generates a net spin triplet polarization $\mathbf{S}_i(\mathbf{k}) = i \langle \mathbf{d}_k \times \mathbf{d}_k^* \rangle$. This term vanishes in the absence of Kondo hybridization. With Kondo hybridization present, the pair-breaking from this term is governed by the interaction energy $\mathbf{S}_i \cdot \mathbf{b}$. It stabilizes superconductivity when $\langle \mathbf{S}_i \rangle$ is (more) anti-parallel to the magnetic field.

VI. CONCLUSION

Inspired by the intriguing $B - T$ phase diagram in systems like engineered Co-NbSe₂ and U-based triplet superconductors, we extend the periodic Anderson model to the case of spin triplet superconductors including both magnetic fields and spin-orbit coupling. Using the Green's function formu-

lation, we obtain the linearized gap equation for the superconducting transition. We find a Kondo resistive state existing below the superconducting phase for both singlet and triplet superconductors that is characterized by small impurity energy $|\varepsilon_f|$. Conversely, in cases of large $|\varepsilon_f|$, the Kondo temperature is larger than the superconducting T_c , resulting in a single critical temperature. While singlet pair-breaking is isotropic with the applied magnetic field direction, triplet superconductivity is strongly field anisotropic, remaining superconducting unless $\mathbf{B} \parallel \mathbf{d}_k$ for all \mathbf{k} . However, including an antisymmetric spin-orbit coupling imposes a paramagnetic limit to triplet superconductivity provided $\mathbf{B} \cdot \mathbf{d}_k \neq 0$ for any \mathbf{k} . Our study illustrates how the Kondo interaction stabilizes the non-unitary triplet order parameter, that is intricately linked to both \mathbf{B} and γ_k . Beyond exploring hypothetical combinations of order parameters, magnetic impurities and spin-orbit interaction, we also directly apply our framework to two known Kondo superconductors including UTe₂ and URhGe, as well as the engineered Co-NbSe₂. Our theoretical framework can provide good qualitative agreement with the observed phase diagrams in these different materials. This highlights the pivotal role played by the Kondo interaction in such magnetic superconductors.

ACKNOWLEDGMENTS

We thank Sheng Ran for helpful comments. This work was supported by the Singapore National Research Foundation Investigator Award (NRF-NRFI06-2020-0003). BÖ acknowledges support from the Singapore NRF Investigatorship (Grant No. NRF-NRFI2018-8), Competitive Research Programme (Grant No. NRF-CRP22-2019-8), and MOE-AcRF-Tier 2 (Grant No. MOE-T2EP50220-0017).

Appendix A: Normal state Green's function

In this Appendix we provide a detailed derivation of the Green's functions. The Green's functions in the imaginary-time momentum space are defined as [46]

$$G_{\mathcal{A}\mathcal{B}}^{s_1 s_2}(\mathbf{k}, \tau) = -\langle T_\tau \mathcal{A}_{\mathbf{k}s_1}(\tau) \mathcal{B}_{\mathbf{k}s_2}^\dagger(0) \rangle, \quad (\text{A1})$$

where \mathcal{A} and \mathcal{B} represent conduction electron c or localized electron f operators. s_1 and s_2 are spin indices. After transforming to Matsubara frequencies, Green's function can be obtained by solving the Dyson equation $(g^{-1} - \mathcal{V})G = I$, which is

$$\begin{pmatrix} i\omega_n - \varepsilon_f - \mathbf{B} \cdot \boldsymbol{\sigma} & -\sqrt{x}V \\ -\sqrt{x}V & i\omega_n - \varepsilon_k - (\gamma_k + \mathbf{B}) \cdot \boldsymbol{\sigma} \end{pmatrix} \times \begin{pmatrix} G_{ff} & G_{cf} \\ G_{fc} & G_{cc} \end{pmatrix} = I_{4 \times 4}. \quad (\text{A2})$$

The Green's function for conduction electrons is obtained as

$$G_{cc}(\mathbf{k}, i\omega_n) = G_+(\mathbf{k}, i\omega_n) + \hat{b} \cdot \boldsymbol{\sigma} G_-(\mathbf{k}, i\omega_n), \quad (\text{A3})$$

with G_+ and G_- given by

$$G_+(\mathbf{k}, i\omega_n) = \frac{i\omega_n - \varepsilon_{\mathbf{k}} + xV^2 \frac{(\varepsilon_f - i\omega_n)}{(\varepsilon_f - i\omega_n)^2 - B^2}}{(\varepsilon_{\mathbf{k}} - \xi_{\mathbf{k}}^+)(\varepsilon_{\mathbf{k}} - \xi_{\mathbf{k}}^-)}, \quad (\text{A4})$$

$$G_-(\mathbf{k}, i\omega_n) = \frac{b}{(\varepsilon_{\mathbf{k}} - \xi_{\mathbf{k}}^+)(\varepsilon_{\mathbf{k}} - \xi_{\mathbf{k}}^-)}. \quad (\text{A5})$$

The poles of the Green's function are written as

$$\xi_{\mathbf{k}}^{\pm} = i\omega_n + xV^2 \frac{(\varepsilon_f - i\omega_n)}{(\varepsilon_f - i\omega_n)^2 - B^2} \pm b. \quad (\text{A6})$$

The Fermi surface splits into two different sheets with the presence of a magnetic field, hybridization, and ASOC.

Appendix B: Linearized gap equation

In this section, we solve the linearized gap equation. Eq. (7) gives rise to

$$\psi_{\mathbf{p}} = -T \sum_{n\mathbf{k}} V_{\mathbf{p}\mathbf{k}} \left[(G_+G_+ - G_-G_- \hat{b} \cdot \hat{b}) \psi_{\mathbf{k}} + (G_-G_+ \hat{b} - G_+G_- \hat{b} + iG_-G_- (\hat{b} \times \hat{b})) \cdot \mathbf{d}_{\mathbf{k}} \right], \quad (\text{B1})$$

$$\mathbf{d}_{\mathbf{k}} = -T \sum_{n\mathbf{k}} V_{\mathbf{p}\mathbf{k}} \left[(G_-G_+ \hat{b} - G_+G_- \hat{b} - iG_-G_- (\hat{b} \times \hat{b})) \psi_{\mathbf{k}} + (G_+G_+ + G_-G_- \hat{b} \cdot \hat{b}) \mathbf{d}_{\mathbf{k}} + i(G_-G_+ \hat{b} + G_+G_- \hat{b}) \times \mathbf{d}_{\mathbf{k}} - G_-G_- ((\mathbf{d}_{\mathbf{k}} \cdot \hat{b}) \hat{b} + (\mathbf{d}_{\mathbf{k}} \cdot \hat{b}) \hat{b}) \right], \quad (\text{B2})$$

Here we use the notation that $G_{\delta}G_{\eta} = G_{\delta}(\mathbf{k}, i\omega_n)G_{\eta}(-\mathbf{k}, -i\omega_n)$ with $\delta, \eta = \pm$. The singlet and triplet gap equations are weakly coupled to each other. However, this coupling depends on the degree of particle-hole asymmetry and is of the order $|\gamma_{\mathbf{k}}|/\varepsilon_F \ll 1$ (ε_F is Fermi energy) [49]. This coupling

becomes exactly zero under our spherical Fermi surface assumption. We therefore ignore this coupling and solve singlet and triplet gap equations separately. The singlet and triplet gap functions are written as [46]

$$\psi_{\mathbf{k}} = \sum_m c_m Y_{lm}(\Omega_{\mathbf{k}}), \quad l \in \text{even},$$

$$\mathbf{d}_{\mathbf{k}} = \sum_{m,\hat{n}} c_{m,\hat{n}} Y_{lm}(\Omega_{\mathbf{k}}) \hat{n}, \quad l \in \text{odd}. \quad (\text{B3})$$

Using the potential $V_{\mathbf{p}\mathbf{k}} = -\sum_{l=0}^{\infty} 4\pi V_l \sum_m Y_{lm}(\Omega_{\mathbf{p}}) Y_{lm}^*(\Omega_{\mathbf{k}})$ [47, 48], Eqs. (B1) and (B2) are simplified to

$$\frac{1}{V_{l \in \text{even}}} = T_c \sum_{n\mathbf{k}} [G_+G_+ - G_-G_- \hat{b} \cdot \hat{b}] |\hat{\psi}_{\mathbf{k}}|^2, \quad (\text{B4})$$

$$\frac{1}{V_{l \in \text{odd}}} = T_c \sum_{n\mathbf{k}} \left[(G_+G_+ + G_-G_- \hat{b} \cdot \hat{b}) |\hat{\mathbf{d}}_{\mathbf{k}}|^2 + i(G_-G_+ \hat{b} + G_+G_- \hat{b}) \cdot (\hat{\mathbf{d}}_{\mathbf{k}} \times \hat{\mathbf{d}}_{\mathbf{k}}^*) - 2G_-G_- (\hat{\mathbf{d}}_{\mathbf{k}} \cdot \hat{b}) (\hat{\mathbf{d}}_{\mathbf{k}}^* \cdot \hat{b}) \right]. \quad (\text{B5})$$

We then calculate the superconducting transition temperature T_c for singlet pairing and triplet pairing by evaluating the Cooper diagram [6, 68]. We introduce the bare superconducting critical temperature T_{c0} without magnetic field, f -electron or ASOC. The gap equations for T_{c0} are

$$\frac{1}{V_{l \in \text{even}}} = T_{c0} \sum_{n\mathbf{k}} g_{cc}(\mathbf{k}, i\omega_n) g_{cc}(-\mathbf{k}, -i\omega_n) |\hat{\psi}_{\mathbf{k}}|^2, \quad (\text{B6})$$

$$\frac{1}{V_{l \in \text{odd}}} = T_{c0} \sum_{n\mathbf{k}} g_{cc}(\mathbf{k}, i\omega_n) g_{cc}(-\mathbf{k}, -i\omega_n) |\hat{\mathbf{d}}_{\mathbf{k}}|^2, \quad (\text{B7})$$

where $g_{cc}^{-1}(\mathbf{k}, i\omega_n) = i\omega_n - \varepsilon_{\mathbf{k}}$ is the bare Green's function. By combining Eqs. (B4) and (B6) (Eqs. (B5) and (B7)) for singlet (triplet), and taking into account the frequency cutoff ω_D , we finally obtain the pair-breaking equation for T_c , which is given in Eq. (8).

-
- [1] G. Riblet and K. Winzer, Vanishing of superconductivity below a second transition temperature in $(\text{La}_{1-x}\text{Ce}_x)\text{Al}_2$ alloys due to the kondo effect, *Solid State Communications* **9**, 1663 (1971).
- [2] M. Maple, W. Fertig, A. Mota, L. DeLong, D. Wohlleben, and R. Fitzgerald, The re-entrant superconducting-normal phase boundary of the Kondo system $(\text{La}, \text{Ce})\text{Al}_2$, *Solid State Communications* **11**, 829 (1972).
- [3] J. Huber, W. Fertig, and M. Maple, Superconducting—normal phase boundaries of $(\text{La}, \text{Th})\text{Ce}$ systems, *Solid State Communications* **15**, 453 (1974).
- [4] K. Winzer, Evidence for a three tc behavior of the Kondo superconductor $(\text{La}, \text{Y})\text{Ce}$, *Solid State Communications* **24**, 551 (1977).
- [5] E. Müller-Hartmann and J. Zittartz, Kondo effect in superconductors, *Physical Review Letters* **26**, 428 (1971).
- [6] V. Barzykin and L. P. Gor'kov, Competition between phonon superconductivity and Kondo screening in mixed valence and heavy fermion compounds, *Physical Review B* **71**, 214521 (2005).
- [7] M. Sato and Y. Ando, Topological superconductors: a review, *Reports on Progress in Physics* **80**, 076501 (2017).
- [8] D. Aoki, K. Ishida, and J. Flouquet, Review of U-based ferromagnetic superconductors: Comparison between UGe_2 , URhGe , and UCoGe , *Journal of the Physical Society of Japan* **88**, 022001 (2019).
- [9] J. Ishizuka, S. Sumita, A. Daido, and Y. Yanase, Insulator-metal transition and topological superconductivity in UTe_2 from a first-principles calculation, *Physical Review Letters* **123**, 217001 (2019).
- [10] T. Shishidou, H. G. Suh, P. M. R. Brydon, M. Weinert, and D. F. Agterberg, Topological band and superconductivity in UTe_2 ,

- Phys. Rev. B* **103**, 104504 (2021).
- [11] A. Aishwarya, J. May-Mann, A. Raghavan, L. Nie, M. Romanelli, S. Ran, S. R. Saha, J. Paglione, N. P. Butch, E. Fradkin, and V. Madhavan, Magnetic-field-sensitive charge density waves in the superconductor UTe_2 , *Nature* **618**, 928 (2023).
- [12] S. Ran, C. Eckberg, Q.-P. Ding, Y. Furukawa, T. Metz, S. R. Saha, I.-L. Liu, M. Zic, H. Kim, J. Paglione, and N. P. Butch, Nearly ferromagnetic spin-triplet superconductivity, *Science* **365**, 684 (2019).
- [13] L. Jiao, S. Howard, S. Ran, Z. Wang, J. O. Rodriguez, M. Sigrist, Z. Wang, N. P. Butch, and V. Madhavan, Chiral superconductivity in heavy-fermion metal UTe_2 , *Nature* **579**, 523 (2020).
- [14] D. Aoki, J.-P. Brison, J. Flouquet, K. Ishida, G. Knebel, Y. Tokunaga, and Y. Yanase, Unconventional superconductivity in UTe_2 , *Journal of Physics: Condensed Matter* **34**, 243002 (2022).
- [15] Y.-Y. Chang, K. Van Nguyen, K.-L. Chen, Y.-W. Lu, C.-Y. Mou, and C.-H. Chung, Correlation-driven topological Kondo superconductors, *Communications Physics* **7**, 253 (2024).
- [16] K. Suzuki and K. Hattori, Ground-state phase diagram of the $S = 1$ one-dimensional Kondo lattice model with a uniaxial anisotropy under transverse fields, *Journal of the Physical Society of Japan* **88**, 024707 (2019).
- [17] K. Suzuki and K. Hattori, Superconducting correlations in the one-dimensional Kondo lattice models under magnetic fields, *Journal of the Physical Society of Japan* **89**, 034703 (2020).
- [18] B. Kang, S. Choi, and H. Kim, Orbital selective Kondo effect in heavy fermion superconductor UTe_2 , *npj Quantum Materials* **7**, 64 (2022).
- [19] C. Thomas, S. Burdin, and C. Lacroix, Metamagnetic transition in the two f orbitals Kondo lattice model, *Journal of Physics: Condensed Matter* **35**, 445601 (2023).
- [20] R. Troć, R. Wawryk, W. Miiller, H. Misiorek, and M. Samsel-Czekala, Bulk properties of the UCoGe Kondo-like system, *Philosophical Magazine* **90**, 2249 (2010).
- [21] N. P. Butch, S. Ran, S. R. Saha, P. M. Neves, M. P. Zic, J. Paglione, S. Gladchenko, Q. Ye, and J. A. Rodriguez-Rivera, Symmetry of magnetic correlations in spin-triplet superconductor UTe_2 , *npj Quantum Materials* **7**, 39 (2022).
- [22] F. Lévy, I. Sheikin, B. Grenier, and A. D. Huxley, Magnetic field-induced superconductivity in the ferromagnet URhGe , *Science* **309**, 1343 (2005).
- [23] D. Aoki, T. D. Matsuda, V. Taufour, E. Hassinger, G. Knebel, and J. Flouquet, Extremely large and anisotropic upper critical field and the ferromagnetic instability in UCoGe , *Journal of the Physical Society of Japan* **78**, 113709 (2009).
- [24] G. Knebel, W. Knafo, A. Pourret, Q. Niu, M. Vališka, D. Braithwaite, G. Lapertot, M. Nardone, A. Zitouni, S. Mishra, I. Sheikin, G. Seyfarth, J.-P. Brison, D. Aoki, and J. Flouquet, Field-reentrant superconductivity close to a metamagnetic transition in the heavy-fermion superconductor UTe_2 , *Journal of the Physical Society of Japan* **88**, 063707 (2019).
- [25] D. Aoki, F. Honda, G. Knebel, D. Braithwaite, A. Nakamura, D. Li, Y. Homma, Y. Shimizu, Y. J. Sato, J.-P. Brison, and J. Flouquet, Multiple superconducting phases and unusual enhancement of the upper critical field in UTe_2 , *Journal of the Physical Society of Japan* **89**, 053705 (2020).
- [26] T. R. Devidas, T. Dvir, E. Rossi, and H. Steinberg, Kondo effect in defect-bound quantum dots coupled to NbSe_2 , *Phys. Rev. B* **107**, 094502 (2023).
- [27] W. Wan, R. Harsh, A. Meninno, P. Dreher, S. Sajan, H. Guo, I. Errea, F. de Juan, and M. M. Ugeda, Evidence for ground state coherence in a two-dimensional Kondo lattice, *Nature communications* **14**, 7005 (2023).
- [28] M. Phillips and V. Aji, Kondo screening in two-dimensional p -type transition-metal dichalcogenides, *Phys. Rev. B* **95**, 075103 (2017).
- [29] D. Sticlet and C. Morari, Topological superconductivity from magnetic impurities on monolayer NbSe_2 , *Physical Review B* **100**, 075420 (2019).
- [30] Y. Zhang, L. Li, J.-H. Sun, D.-H. Xu, R. Lü, H.-G. Luo, and W.-Q. Chen, Kondo effect in monolayer transition metal dichalcogenide Ising superconductors, *Phys. Rev. B* **101**, 035124 (2020).
- [31] T. Qu, S. Jin, F. Hou, D. Fu, J. Huang, D. F. C. Wei, X. Chang, K. Watanabe, T. Taniguchi, J. Lin, S. Adam, and B. Özyilmaz, Ferromagnetic superconductivity in two-dimensional niobium diselenide, *arXiv preprint arXiv:2306.06659* (2023).
- [32] L. P. Gor'kov and E. I. Rashba, Superconducting 2D system with lifted spin degeneracy: mixed singlet-triplet state, *Physical Review Letters* **87**, 037004 (2001).
- [33] D. Möckli and M. Khodas, Robust parity-mixed superconductivity in disordered monolayer transition metal dichalcogenides, *Physical Review B* **98**, 144518 (2018).
- [34] W.-Y. He, B. T. Zhou, J. J. He, N. F. Yuan, T. Zhang, and K. T. Law, Magnetic field driven nodal topological superconductivity in monolayer transition metal dichalcogenides, *Communications Physics* **1**, 40 (2018).
- [35] D. Wickramaratne, S. Khmelevskiy, D. F. Agterberg, and I. I. Mazin, Ising superconductivity and magnetism in NbSe_2 , *Phys. Rev. X* **10**, 041003 (2020).
- [36] A. Hamill, B. Heischmidt, E. Sohn, D. Shaffer, K.-T. Tsai, X. Zhang, X. Xi, A. Suslov, H. Berger, L. Forró, F. J. Burnell, J. Shan, K. F. Mak, R. M. Fernandes, K. Wang, and V. S. Pribiag, Two-fold symmetric superconductivity in few-layer NbSe_2 , *Nature physics* **17**, 949 (2021).
- [37] P. Wan, O. Zheliuk, N. F. Yuan, X. Peng, L. Zhang, M. Liang, U. Zeitler, S. Wiedmann, N. E. Hussey, T. T. Palstra, and J. Ye, Orbital fulde-ferrell-larkin-ovchinnikov state in an Ising superconductor, *Nature* **619**, 46 (2023).
- [38] F. Ara, S. M. Fakruddin Shahed, M. I. Hossain, K. Katoh, M. Yamashita, and T. Komeda, Control of the magnetic interaction between single-molecule magnet TbPc_2 and superconductor NbSe_2 surface by an intercalated Co atom, *Nano Letters* **23**, 6900 (2023).
- [39] K. Machida, Nonunitary triplet superconductivity tuned by field-controlled magnetization: URhGe , UCoGe , and UTe_2 , *Physical Review B* **104**, 014514 (2021).
- [40] K. A. Gschneidner, J.-C. G. Bunzli, and V. K. Pecharsky, *Handbook on the physics and chemistry of rare earths: optical spectroscopy* (Elsevier, 2011).
- [41] T. Schäfer, A. A. Katanin, M. Kitatani, A. Toschi, and K. Held, Quantum criticality in the two-dimensional periodic Anderson model, *Phys. Rev. Lett.* **122**, 227201 (2019).
- [42] T. Miyao and H. Tominaga, Ground state properties of the periodic Anderson model with electron-phonon interactions, *Annals of Physics* **455**, 169381 (2023).
- [43] T. Rice and K. Ueda, Gutzwiller variational approximation to the heavy-fermion ground state of the periodic Anderson model, *Physical review letters* **55**, 995 (1985).
- [44] B. Velický, S. Kirkpatrick, and H. Ehrenreich, Single-site approximations in the electronic theory of simple binary alloys, *Phys. Rev.* **175**, 747 (1968).
- [45] A.-B. Chen, Electronic structure of disordered alloys—iteration scheme converging to the coherent-potential approximation, *Phys. Rev. B* **7**, 2230 (1973).

- [46] M. Sigrist and K. Ueda, Phenomenological theory of unconventional superconductivity, *Reviews of Modern physics* **63**, 239 (1991).
- [47] P. W. Anderson and P. Morel, Generalized bardeen-cooper-schrieffer states and the proposed low-temperature phase of liquid He³, *Physical Review* **123**, 1911 (1961).
- [48] R. Balian and N. Werthamer, Superconductivity with pairs in a relative p wave, *Physical review* **131**, 1553 (1963).
- [49] P. Frigeri, D. Agterberg, A. Koga, and M. Sigrist, Superconductivity without inversion symmetry: MnSi versus CePt₃Si, *Physical review letters* **92**, 097001 (2004).
- [50] X. Xi, Z. Wang, W. Zhao, J.-H. Park, K. T. Law, H. Berger, L. Forró, J. Shan, and K. F. Mak, Ising pairing in superconducting NbSe₂ atomic layers, *Nature Physics* **12**, 139 (2016).
- [51] A. A. Abrikosov and L. P. Gor'kov, Contribution to the theory of superconducting alloys with paramagnetic impurities, *Sov Phys JETP* **12**, 1243 (1961).
- [52] S. Kittaka, Y. Shimizu, T. Sakakibara, A. Nakamura, D. Li, Y. Homma, F. Honda, D. Aoki, and K. Machida, Orientation of point nodes and nonunitary triplet pairing tuned by the easy-axis magnetization in UTe₂, *Physical Review Research* **2**, 032014 (2020).
- [53] I. M. Hayes, D. S. Wei, T. Metz, J. Zhang, Y. S. Eo, S. Ran, S. R. Saha, J. Collini, N. P. Butch, D. F. Agterberg, A. Kapitulnik, and J. Paglione, Multicomponent superconducting order parameter in UTe₂, *Science* **373**, 797 (2021).
- [54] H. Fujibayashi, G. Nakamine, K. Kinjo, S. Kitagawa, K. Ishida, Y. Tokunaga, H. Sakai, S. Kambe, A. Nakamura, Y. Shimizu, Y. Homma, D. Li, F. Honda, and D. Aoki, Superconducting order parameter in UTe₂ determined by Knight shift measurement, *journal of the physical society of japan* **91**, 043705 (2022).
- [55] H. Matsumura, H. Fujibayashi, K. Kinjo, S. Kitagawa, K. Ishida, Y. Tokunaga, H. Sakai, S. Kambe, A. Nakamura, Y. Shimizu, Y. Homma, D. Li, F. Honda, and D. Aoki, Large reduction in the a-axis Knight shift on UTe₂ with T_c = 2.1 K, *Journal of the Physical Society of Japan* **92**, 063701 (2023).
- [56] F. Theuss, A. Shragai, G. Grissonnanche, I. M. Hayes, S. R. Saha, Y. S. Eo, A. Suarez, T. Shishidou, N. P. Butch, J. Paglione, *et al.*, Single-component superconductivity in UTe₂ at ambient pressure, *Nature Physics* , 1 (2024).
- [57] S. Lee, A. J. Woods, P. F. S. Rosa, S. M. Thomas, E. D. Bauer, S.-Z. Lin, and R. Movshovich, [Anisotropic field-induced changes in the superconducting order parameter of UTe₂](#) (2023), [arXiv:2310.04938 \[cond-mat.supr-con\]](#).
- [58] H. S. Røising, M. Geier, A. Kreisel, and B. M. Andersen, Thermodynamic transitions and topology of spin-triplet superconductivity: Application to UTe₂, *Physical Review B* **109**, 054521 (2024).
- [59] G. Nakamine, K. Kinjo, S. Kitagawa, K. Ishida, Y. Tokunaga, H. Sakai, S. Kambe, A. Nakamura, Y. Shimizu, Y. Homma, D. Li, F. Honda, and D. Aoki, Anisotropic response of spin susceptibility in the superconducting state of UTe₂ probed with ¹²⁵Te-NMR measurement, *Physical Review B* **103**, L100503 (2021).
- [60] G. Nakamine, K. Kinjo, S. Kitagawa, K. Ishida, Y. Tokunaga, H. Sakai, S. Kambe, A. Nakamura, Y. Shimizu, Y. Homma, D. Li, F. Honda, and D. Aoki, Inhomogeneous superconducting state probed by ¹²⁵Te NMR on UTe₂, *journal of the physical society of japan* **90**, 064709 (2021).
- [61] D. Aoki, A. Nakamura, F. Honda, D. Li, Y. Homma, Y. Shimizu, Y. J. Sato, G. Knebel, J.-P. Brison, A. Pourret, D. Braithwaite, G. Lapertot, Q. Niu, M. Vališka, H. Harima, and J. Flouquet, Unconventional superconductivity in heavy fermion UTe₂, *journal of the physical society of japan* **88**, 043702 (2019).
- [62] J. Ishizuka and Y. Yanase, Periodic Anderson model for magnetism and superconductivity in UTe₂, *Physical Review B* **103**, 094504 (2021).
- [63] V. P. Mineev, Superconducting states in ferromagnetic metals, *Phys. Rev. B* **66**, 134504 (2002).
- [64] A. Huxley, V. Mineev, B. Grenier, E. Ressouche, D. Aoki, J. Brison, and J. Flouquet, Order parameter symmetry in the superconducting ferromagnets UGe₂ and URhGe, *Physica C: Superconductivity* **403**, 9 (2004).
- [65] Y. Yanase, Magneto-electric effect in three-dimensional coupled zigzag chains, *Journal of the Physical Society of Japan* **83**, 014703 (2014).
- [66] Y. Tada, S. Takayoshi, and S. Fujimoto, Magnetism and superconductivity in ferromagnetic heavy-fermion system UCoGe under in-plane magnetic fields, *Physical Review B* **93**, 174512 (2016).
- [67] M. Diviš, L. Sandratskii, M. Richter, P. Mohn, and P. Novák, Magnetism of URhSi and URhGe: a density functional study, *Journal of alloys and compounds* **337**, 48 (2002).
- [68] P.-G. De Gennes, *Superconductivity of metals and alloys* (CRC press, 2018).